# Functional Terpolymers Containing Vinylphosphonic Acid: The Synthesis and Characterization of Poly(Vinylphosphonic Acid-*co*-Styrene-*co*-Maleic Anhydride)

**Serap Kavlak,[1] Ali Güner,[1] Zakir M. O. Rzayev[2]**

[1]*Department of Chemistry, Faculty of Science, Hacettepe University, Beytepe, Ankara 06800, Turkey*
[2]*Department of Chemical Engineering, Faculty of Engineering, Hacettepe University, Beytepe, Ankara 06800, Turkey*

Received 22 February 2011; accepted 27 October 2011
DOI 10.1002/app.36522
Published online in Wiley Online Library (wileyonlinelibrary.com).

**ABSTRACT:** Novel functional temperature-sensitive amphiphilic P-containing polymers were synthesized by complex-radical ternary polymerization of vinylphosphonic acid (VPA), styrene (S), and maleic anhydride (MA). Charge transfer complexes (CTCs), complex-formation constants ($K_c$) between acceptor and donor monomer systems and the complexed monomer reactivity ratios were investigated by $^1$H-NMR analysis. Contrary to theoretical predictions, the VPA...S complex is more active as compared to MA...S complex in the ternary system since VPA monomer can form the CTC both with S monomer and strong H-bonded complex with MA monomer. The terpolymer compositions, characterizations, and structure–property relationships of a series of poly(VPA-*co*-S-*co*-MA)s were investigated by GPC, FTIR, Raman, $^1$H-NMR, $^{13}$C-NMR, DEPT-135, $^{31}$P-NMR, TGA-DSC, DMA, XRD, viscometry, and titration. © 2012 Wiley Periodicals, Inc. J Appl Polym Sci 000: 000–000, 2012

**Key words:** complex-formation; structure–property relations; monomer reactivity ratios; radical polymerization; thermal properties

## INTRODUCTION

During the last years, there exists a strong demand for new and improved functional polymers with specific properties. Functional groups or introduction of small ionic groups into the polymer can modify physical and rheological properties.[1–4] Functionalized polymers have wide applications for various biological and technological purposes. Synthetic polymers containing phosphonic acid groups have received special attention due to the important applications in the field of dental and orthopedic biomaterials because of their calcium binding affinity.[5,6] Dibasic phosphonic acid groups have been used as cation exchange groups in the studies on cation-exchange resins[7,8] and fuel cell membranes.[9,10] Phosphorus compounds are also used as flame-retardant additives in polymers. Effects of incorporating phosphorus-containing comonomer units on the flame-retardance particularly of polystyrene and of poly(methyl methacrylate) have been established.[11]

Complex-radical copolymerization of electron-donor and electron-acceptor binary and ternary monomer systems is an effective method for the synthesis of functional macromolecules with given composition, structure, and properties.[12–18] In some earlier publications, a number of systematic studies were carried out for the terpolymerization of maleic anhydride, styrene, and donor- or acceptor-type monomers such as unsaturated epoxides,[18] acrylics,[19,20] citraconic anhydride,[21] certain maleimides,[22] and *N*-vinyl pyrrolidone.[23]

Ternary monomer systems in terms of the conjugation type in monomer molecule, electron-donor (D) and electron-acceptor (A) behavior of monomers, homopolymerizability of individual comonomers in the chosen terpolymerization conditions and the mechanism of chain growth, can be classified by the following groups: (1) $D_1-D_2-D_3$, (2) $A_1-A_2-A_3$, (3) $D_1-A-D_2$, and (4) $A_1-D-A_2$. In the chosen terpolymerization conditions (1) and (2) groups may be comprised the following cases: (a) all three comonomers can be homopolymerized, (b) two monomers are homopolymerized, (c) only one monomer is homopolymerized, and (d) all three comonomers are not homopolymerized. Complex-formation does not occur in these monomer systems of which have similar type of double bond conjugation. Therefore,

*Correspondence to:* A. Güner (agun@hacettepe.edu.tr).
Contract grant sponsor: The Scientific and Technological Research Council of Turkey (TÜBİTAK); contract grant number: TBAG-106T141.
Contract grant sponsor: Hacettepe University Scientific Research Foundation; contract grant number: BAB-05D11601003.


© 2012 Wiley Periodicals, Inc.

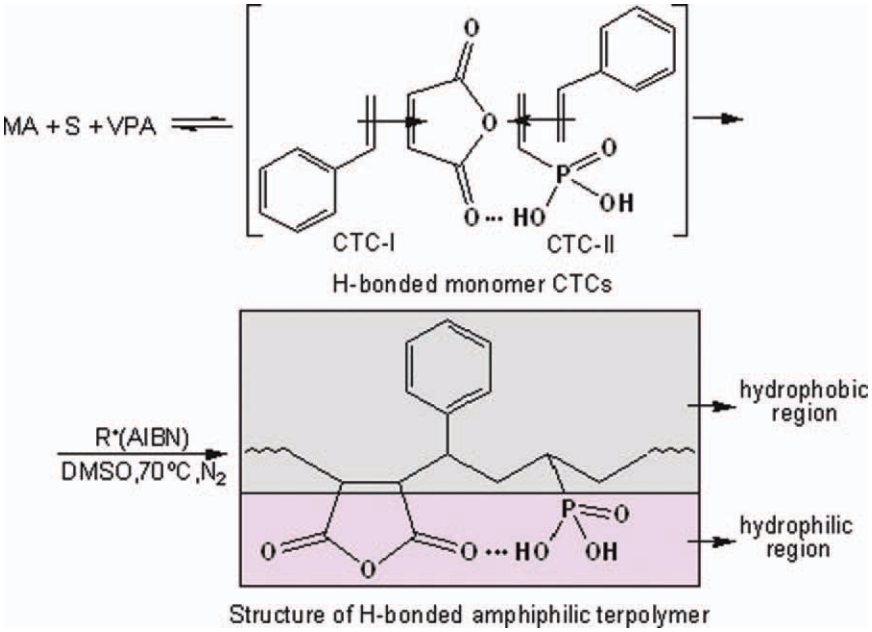


**Scheme 1** Terpolymerization of VPA, S, and MA via monomer CTCs. [Color figure can be viewed in the online issue, which is available at wileyonlinelibrary.com.]

reaction yielded usual equations of random copolymerization and differed by complexity in term of the "controlling" by radical reactions of the chain growth. The groups of (3) and (4) may also comprise all the cases as in (1) and (2) ternary monomer systems. However, these ternary systems comprise only the donor-acceptor monomers which can be presented by two $D_1 \ldots A$ and $D_2 \ldots A$ complexes for (3) and $A_1 \ldots D$ and $A_2 \ldots D$ complexes for (4) systems, respectively, in initiation, propagation termination and chain transfer reactions. These systems may also include the monomers containing the functional groups with H-bonded and/or coordinated complexes in monomer feed. Number of the elementary chain growth reactions in these ternary systems depends on the complex formation and homopolymerization properties of comonomers in given radical terpolymerization conditions. Ternary monomer systems containing maleic anhydride and its isostructural analogues, as strong electron-acceptor monomers differ from other monomer systems in that the radical ternary polymerizations occur via both free and complexed monomers. These monomer systems were predominantly described as a binary copolymerization of two complexed monomers.[13,14,18,24–28]

In this study, $A_1-D-A_2$ monomer system was investigated. New P-containing functional terpolymers of vinylphosphonic acid (VPA as an electron-acceptor monomer), styrene (S as an electron-donor monomer) and maleic anhydride (MA as an electron-acceptor monomer) were synthesized by complex-radical terpolymerization method at different monomer feed ratios. Charge transfer complexes (CTCs) formed between acceptor and donor monomer systems were investigated and complex formation constant ($K_c$) values were determined with $^1$H-NMR spectroscopy. The monomer reactivity ratios of CTCs were found by $^1$H-NMR analysis. Identification of the structures, terpolymer compositions, and characterization of the terpolymers obtained from different monomer feed ratios were investigated by FTIR, Raman, $^1$H-NMR, $^{13}$C-NMR, DEPT-135, $^{31}$P-NMR spectroscopy, viscometry, DSC, TGA, DMA, GPC, and XRD methods.

The synthesis of terpolymers can be represented schematically as follows (Scheme 1).

## EXPERIMENTAL PART

### Materials

VPA (Fluka) monomer was used without further any purification. mp. 41–45°C, $d_4^{20}$ 1.409, $n_D^{20}$ 1.473. Raman spectrum ($cm^{-1}$): 3090 (O—H stretching band), 2876 (C—H stretching vibration), 2374 (P—OH stretching), 1224 (P=O stretching), 936 (O—P—O band). $^1$H-NMR spectrum (DMSO-$d_6$): $\delta$ = 8.50 (s, OH, 2H), 6.18–6.05 (m, CH=, 1H) 5.99–5.78 (q, $H_2C$=, 2H). S (Aldrich) monomer was purified before use by distillation under vacuum. MA (Aldrich) monomer was purified before use by recrystallization from anhydrous benzene and dried under vacuum. 2,2′-Azobisisobutyronitrile (AIBN) (Fluka) was recrystallized from methanol and was dried under vacuum. All other solvents and reagents were analytical grade and used as received.

### Complex formations in the monomer systems

$K_c$ for the for the S-MA (at 25°C) and S-VPA (25 and 50°C) complex was determined by the $^1$H-NMR spectroscopy in DMSO-$d_6$; $^1$H-NMR spectra of pure monomers and their mixtures (VPA, MA:S = 1 : 5, 1 : 10, 1 : 20, 1 : 30 mol %) ([S]>>[VPA], [MA]); [VPA, MA] = 0.1 mol $L^{-1}$, [S] = 0.5, 1.0, 2.0, and 3.0 mol $L^{-1}$) with an excess of electron-donor monomer (S) showed an appreciable displacement of chemical shifts of electron-acceptor monomers (MA at 25°C, VPA at 25 and 50°C).

### Synthesis of terpolymers

The radical terpolymerizations of VPA with S and MA at certain monomer feed ratios (10 : 50 : 40, 25 : 50 : 25, 40 : 50 : 10 mol %) were performed in 70 wt % solutions of monomers in DMSO, using AIBN (1.0%, based on the total weight of monomers) as initiator. For polymerizations standard conditions were used as follows: Narrow neck tubes were charged with appropriate quantities of monomers, DMSO and AIBN. To reduce the influence of oxygen, tubes were flushed with nitrogen gas. The solution heated to 70°C and stirred at this temperature for 24 h, at nitrogen atmosphere. At the end of the reaction polymer mixtures were cooled to room temperature and polymers separated by precipitation with methanol, and then washed with several portions of diethyl ether and finally reprecipitated from acetone solution. Resultant polymers were dried under vacuum.

The poly(VPA-*co*-S-*co*-MA)s are systematically named according to the monomer feed ratio of terpolymers are terpolymer-1 (10 : 50 : 40 mol %), terpolymer-2 (25 : 50 : 25 mol %), and terpolymer-3 (40 : 50 : 10 mol %).

### Determination of the complexed monomer reactivity ratios

To determine the reactivity ratios terpolymerizations of VPA with S and MA at certain monomer feed ratios [VPA...S]:[MA...S] = 20 : 80 mol % and [VPA...S]:[MA...S] = 80 : 20 mol % were polymerized to a low conversion at the same conditions. Terpolymerization reactions were performed inside NMR equipment before and after reaction at 70°C for 5.5 h using deuterated DMSO as a solvent. To reduce the influence of oxygen, tubes were flushed with nitrogen gas before polymerization.

### Characterization

The FTIR spectra of monomers were recorded with a Mattson 1000 FTIR spectrometer in the 4000–400 $cm^{-1}$ range by signal averaging a total of 30 scans, the resolution was 4 $cm^{-1}$. Samples were prepared by mixing the polymers with KBr (1 : 9 wt %) powder. The Raman spectra of monomers were obtained with a Jobin-Yvon LabRam HR800 Raman spectrometer equipped with a charge coupled device (CCD) detector using the 632.8 nm line of a He-Ne nm laser. Samples were recorded with a 3 accumulation, 400s (objective 100×, grating 600). To determine the complex formation constants and structural identifications $^1$H-, $^{13}$C-NMR spectra were collected for monomers and monomer pairs using a Bruker 400 MHz NMR spectrometer. For the $^1$H, $^{13}$C analysis TMS was used as the internal standard and for the $^{31}$P-NMR analysis $H_3PO_4$ was used as the internal standard.

Molecular weights, polydispersity index, and radius of gyration values of terpolymers were determined by GPC method in THF at 30°C using PL-GPC 220 GPC equipment. The column oven can comfortably hold two 30 cm GPC columns, refractive index (RI) detector and injection valve, as well as a viscometer and two-angle (15° and 90°) light scattering detector. Polystyrenes with narrow polydispersity index were used for universal calibration.

Thermogravimetric analysis (TGA) of polymers was performed with a Shimadzu TA-60WS thermal analyzer. Thermal degradation of the polymers was investigated under nitrogen atmosphere with a heating rate of 10°C/min from 30 to 500°C. Thermal transitions of the polymers were investigated by Shimadzu DSC-60 Instruments under nitrogen atmosphere with a heating rate of 10°C/min, from 30 to 300°C. Glass transition temperatures were determined from the second heating run as the middle points.

Dynamic mechanic behaviors of terpolymers were performed by TA Q800 dynamic mechanic analyzer (DMA). Mixtures of polymer and $Al_2O_3$ (50 : 50 wt %) were prepared and these powdered mixtures were loaded into the DMA using a powder-holder, which consisted of upper and lower tray of stainless steel. The holder was clamped directly into the DMA dual cantilever rig and tightened 6 PSI torque using the torque tool. The temperature dependence of polymers was measured at a constant frequency ($\omega$ = 1 Hz) using a standard temperature sweep (3°C/min) from −50 to 250°C. These temperature ranges were achieved by initially cooling the DMA using a liquid nitrogen accessory.

The powder diffraction patterns of synthesized samples were recorded using a Rigaku D/MAX 2200 PC X-ray powder diffractometer. The Cu anode X-ray tube way operated at 40 kV and 36 mA in combination with a Ni filter to give monochromatic $CuK_\alpha$ X-rays over the range of $2^\circ \leq 2\theta \leq 60^\circ$.

Viscosity behaviors of terpolymers were performed by Ubbelohde type capillary viscometer at

25 ± 0.1°C. Acid numbers of terpolymers were determined experimentally for each sample by the known titration method.[29]

## RESULTS AND DISCUSSION

### Formation of charge-transfer and H-bonded complexes

In solutions of the complex, there is a rapid exchange between protons in complexed and uncomplexed states and the chemical shift observed for protons on one of the monomers ($\delta_{obs}$) is a weighted average of the shift due to the free molecules ($\delta_f$) and that due to the complex ($\delta_{CTC}$). According to the Hanna-Ashbaugh relation:[30]

$$\frac{1}{\Delta_{obs}} = \frac{1}{K_c[D]_0\Delta_{CTC}} + \frac{1}{\Delta_{CTC}} \quad (1)$$

where $\Delta_{obs} = \delta_{obs} - \delta_f$, $\Delta_{CTC} = \delta_{CTC} - \delta_f$ and $(D)_0$ is concentration of a donor monomer. $^1$H-NMR spectra of pure monomers and their mixtures with an excess of electron-donating monomer (S>>VPA) show an appreciable displacement of chemical shifts of vinylphosphonic acid protons at 25 and 50°C ($\delta_{CH}$ = 6.0519 ppm, $\delta_{CH}$ = 6.0559 ppm) to the weak field ($\delta_{CH}$ = 6.0985–6.2195 ppm, $\delta_{CH}$ = 6.1023–6.2185 ppm) [Fig. 1(a,b)]. The results were summarized in Table I. The changes for chemical shifts with a significant excess of S allow the equilibrium constant ($K_c$) of complexation to be determined. The values of $K_{c1}$ = 0.458 ± 0.1 L mol$^{-1}$ at 25°C and 0.484 ± 0.1 L mol$^{-1}$ at 50°C, for VPA:S, respectively, were found from the graphical relationship $\Delta_{obs}^{-1}$ (ppm$^{-1}$) → 1/$[D]_0$. In this studied system, there are small differences between the two $K_c$ values and it increases with temperature due to the strong intramolecular hydrogen bonding in the monomers. At lower temperature, CTC between VPA…S is smaller resulting from the intramolecular hydrogen bonding between VPA monomer units. At higher temperatures this hydrogen bonding in VPA units is weaker and charge transfer complexes between VPA and S monomers become more active. From the donor–acceptor properties of the studied monomers, it may be predicted that the following equimolar (1 : 1) CTCs and H-bonded complex in the monomer mixtures are formed as shown below (Scheme 2):

MA-S monomer pair is an old but well studied and detailed system for demonstration of the complex-radical mechanism of alternating copolymerization.[20,31] In MA-S system, $^1$H-NMR spectra of pure monomer and their mixtures with an excess of electron-donating monomer (S>>MA) show an appreciable displacement of chemical shifts of maleic anhydride protons at 25°C ($\delta_{CH}$ = 7.475 ppm) to the strong field ($\delta_{CH}$ = 7.475–7.437 ppm) [Fig. 1(c)]. Results are illustrated in Table I. The value of $K_{c2}$ = 0.252 ± 0.1 L mol$^{-1}$ for MA:S at 25°C were found from the graphical relationship $\Delta_{obs}^{-1}$ (ppm$^{-1}$) → 1/$[D]_0$. This result is supported by the good agreement

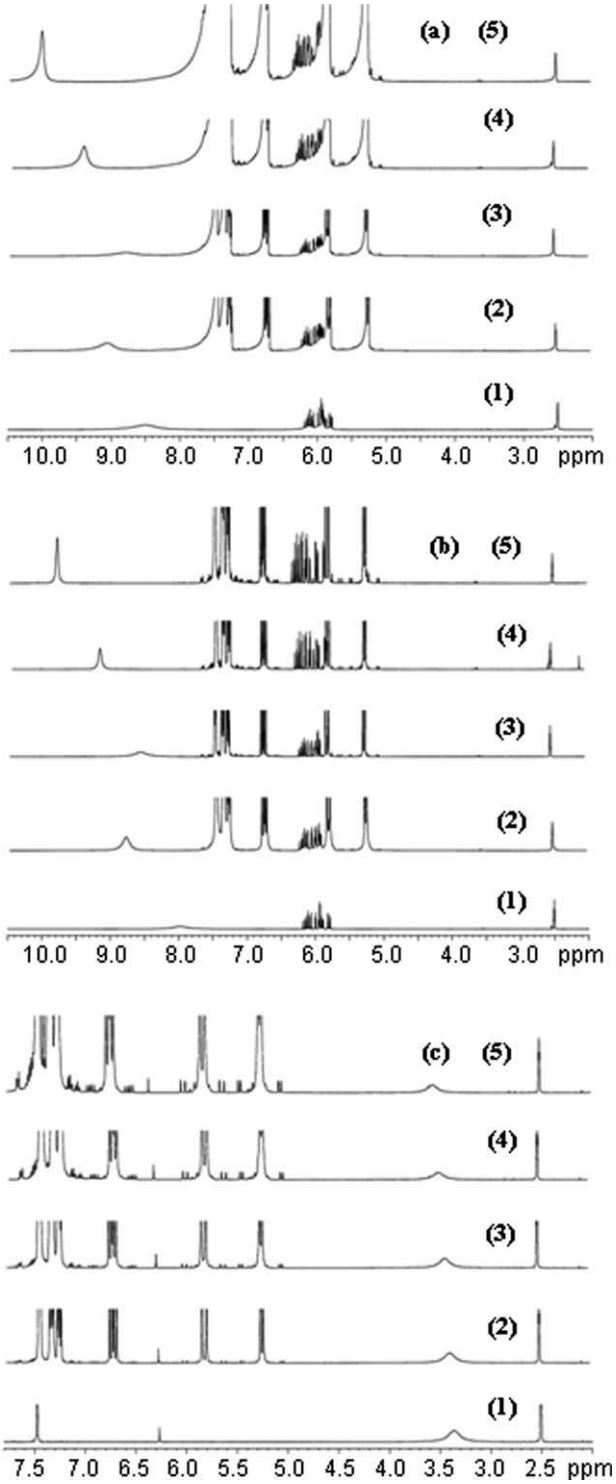


**Figure 1** $^1$H-NMR spectra of VPA:S monomer mixtures with different compositions at 25°C (a), 50°C (b) and MA:S monomer mixtures with different compositions at 25°C (c): (1) 1 : 0, (2) 1 : 5, (3) 1 : 10, (4) 1 : 20, (5) 1 : 30 in DMSO-$d_6$.

**TABLE I**
**Effect of CTC on the Chemical Shifts in the Monomer Systems at 25 and 50°C**

| Monomer feed (mol $L^{-1}$) [VPA] ([MA]) [S] | | $\Delta_{obs}$ (CH=, VPA) 25°C | $\Delta_{obs}$ (CH=, VPA) 50°C | $\Delta_{obs}$ (CH=, MA) 25°C |
|---|---|---|---|---|
| 0.1 | 0.5 | 0.047 | 0.046 | 0.002 |
| 0.1 | 1.0 | 0.062 | 0.061 | 0.005 |
| 0.1 | 2.0 | 0.121 | 0.118 | 0.016 |
| 0.1 | 3.0 | 0.168 | 0.163 | 0.039 |

with the data for this system found in literature. The value of $K_c$ for this complex is reported as 0.29 L $mol^{-1}$ in benzene at 20°C and 0.226 L $mol^{-1}$ in $CDCl_3$ at 27°C,[13,32] 0.34 L $mol^{-1}$ in hexane at 30.1°C and 0.30 L $mol^{-1}$ at 60°C.[31]

### The complexed monomer reactivity ratios

Terpolymerizations of donor and acceptor monomer systems can be described as binary copolymerization system of two different monomer charge transfer complexes and terpolymerizations occurred by the way of both free and complexed monomers. Terpolymerizations were carried out to low conversions (≤10%) to determine the monomer reactivity ratios in the steady-state kinetics by using known modified Jaacks equations[33] and $^1$H-NMR analysis. The Jaacks method was preferentially applied since it involves the use of a large excess of one monomer pair relative to the other one to consider only one growing radical:

$$\log([Am_1]_t/[Am_2]0) = r_{\mathrm{I}}.\log([Am_2]_t/[Am_2]_0) \quad \text{for } [\mathrm{MA}\ldots\mathrm{S}] << [\mathrm{VPA}\ldots\mathrm{S}] \quad (2)$$

$$\log([Am_2]_t/[Am_2]0) = r_{\mathrm{II}}.\log([Am_1]_t/[Am_1]_0) \quad \text{for } [\mathrm{VPA}\ldots\mathrm{S}] << [\mathrm{MA}\ldots\mathrm{S}] \quad (3)$$

where $[Am_i]_0$ and $[Am_i]_t$ are the integral areas of —CH=CH— protons of MA, —$CH_2$=CH— protons of S and —$CH_2$=CH— protons of VPA monomers before and after polymerization at low conversion conditions for a given time $t$, respectively; $[Am_1]_0$ (or $[Am_1]_t$) = ($H_a$ + $H_b$) (for MA), $[Am_2]_0$ (or $[Am_2]_t$) = ($H_a$ + $H_b$) (for S), $[Am_3]_0$ (or $[Am_3]_t$) = ($H_a$ + $H_b$) (for VPA), (Fig. 2, Table II). Analysis of constants of copolymerizations, taking into account the constants of CTC formation, provides that the VPA…S complex is more active in the radical copolymerization as compared with MA…S complex in the VPA-S-MA system: $r_{\mathrm{I}} = r_1(K_{c2}/K_{c1})$ = 1.39, $r_{\mathrm{II}} = r_2(K_{c1}/K_{c2})$ = 0.91; $r_1$ = 2.52, $r_2$ = 0.50 (taking into account $K_{c2}$ and $K_{c1}$ constants). The values of copolymerization constants were obtained by taking into consideration the variation of $K_c$ on the reactivity of the monomers. The chains of the copolymers will be slightly richer in the [MA…S] units due to the higher reactivity of this monomer pair. Product of the reactivity ratios being 1.26; verifies the fact that monomer units are randomly distributed along the chains.

### Structural characterization of terpolymers

Compositions of terpolymers were determined by FTIR spectroscopy. The absorption value ratios between characteristic analytical bands of 1731–1708 $cm^{-1}$ (for MA unit), 700–696 $cm^{-1}$ (for S unit), 948–946 $cm^{-1}$ (for VPA unit) and the least changing absorption band of 541 $cm^{-1}$ as a standard band ($A$ = $\log(I_0/I)$) were used to calculate the terpolymer compositions. Molar fractions (in mol %) of monomer units ($m_1$, $m_2$ and $m_3$) in VPA($M_1$)-S($M_2$)-MA($M_3$) terpolymers using FTIR analysis data are calculated according to the following equations:[34]

$$m_1 = \frac{\Delta A^{948}/M_1}{\Delta A^{1731}/M_3 + \Delta A^{700}/M_2 + \Delta A^{948}/M_1} \times 100 \quad (4)$$

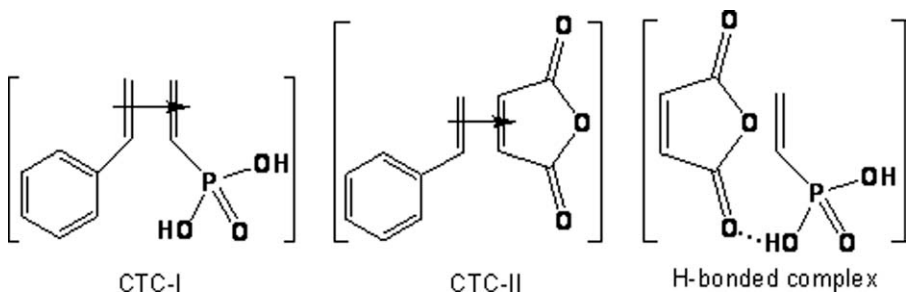


**Scheme 2** Proposed structure of charge-transfer and H-bonded complexes.

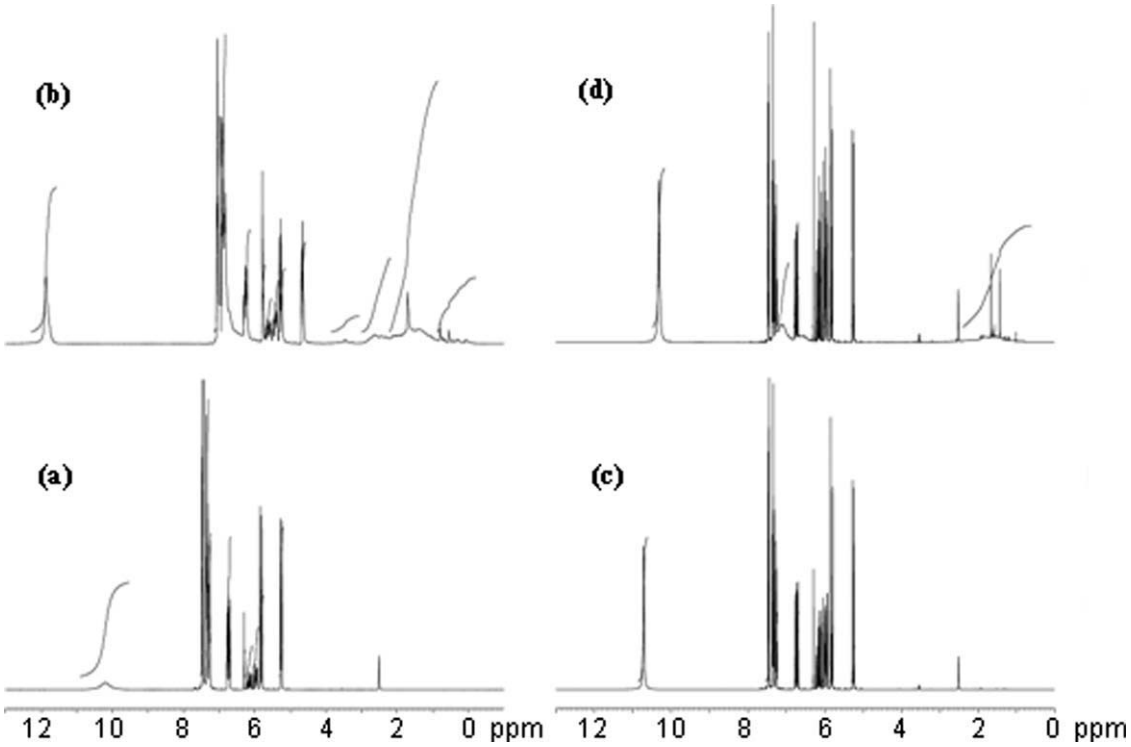


**Figure 2** $^1$H-NMR spectra of monomer mixtures of MA...S : VPA...S = 80 : 20 mol % before (a) and after (b); MA...S : VPA...S = 20 : 80 mol % before (c) and after (d) reaction at 70°C for 5.5 h in DMSO-$d_6$.

$$m_2 = \frac{\Delta A^{700}/M_2}{\Delta A^{1731}/M_3 + \Delta A^{700}/M_2 + \Delta A^{948}/\mathrm{M}_1} \times 100 \quad (5)$$

$$m_3 = \frac{\Delta A^{1731}/M_3}{\Delta A^{1731}/M_3 + \Delta A^{700}/M_2 + \Delta A^{948}/M_1} \times 100 \quad (6)$$

$\Delta A = A^i/A^{541}$ (standard band); $M_1$, $M_2$, and $M_3$ are molecular weights (g/mol) of VPA, S, and MA monomer units, respectively. Compositions of VPA, S, and MA in poly(VPA-*co*-S-*co*-MA)s are summarized in the Table III. To analyze the composition of terpolymers relatively high conversations were used. In this system especially in equimolar composition CTCs can be more effective but in other compositions polymerizations occurred by the way of both free and complexed monomers. On the other hand there are interactions due to the inter- and intramolecular H-bonding between MA and VPA units, respectively in this system. Both the CTC and H-bonded complex significantly influenced the monomer reactivity ratios in terpolymerization. High incorporation of MA may come from these situations.

The molecular weight distribution plots are presented in Figure 3 and the molecular weight averages and polydispersities are summarized in Table IV. Observed unusual lower molecular weight of terpolymer-2 synthesized from equimolar mixture of CTC-I and CTC-II can be explained with the exchange reaction responsible between these different complexes before chain growing reactions which significantly reduce the molecular weight. Polydispersity index for the terpolymers changes from 1.87 to 3.32 and it can be said that polydisperse polymers were obtained. $R_g$ increased with increasing vinylphosphonic acid units in terpolymer. Relatively small $R_g$ values may come from the molecular weight distribution or compact structure resulting from the H-bond formation between molecular interactions.

**TABLE II**
**$^1$H-NMR Analysis Data of VPA/S/MA Monomer Mixtures before and after Terpolymerization for the Determination of the Monomer Reactivity Ratios Using the Modified Jaacks Equations**

| Monomer feed (mol %) | Integral area of VPA —$CH_2$=CH— protons | Integral area of S —$CH_2$=CH— protons | Integral area of MA —CH=CH— protons |
|---|---|---|---|
| [VPA...S] [MA...S] | $[Am_3]_0$ $[Am_3]_t$ | $[Am_2]_0$ $[Am_2]_t$ | $[Am_1]_0$ $[Am_1]_t$ |
| 20 80 | 0.2724 0.1912 | 1.5640 0.7545 | 0.7820 0.3573 |
| 80 20 | 0.3220 0.2762 | 0.4700 0.3085 | 0.2350 0.1543 |

**TABLE III**
**Terpolymer Compositions Determined by FTIR Method**

| Monomer feed (mol %) | | | $\Delta A^{948}$ | $\Delta A^{700}$ | $\Delta A^{1731}$ | Terpolymer composition (mol %) | | |
|---|---|---|---|---|---|---|---|---|
| [VPA] | [S] | [MA] | VPA-unit | S-unit | MA-unit | $m_1$ | $m_2$ | $m_3$ |
| 10 | 50 | 40 | 1.871 | 3.188 | 3.561 | 20.55 | 36.34 | 43.11 |
| 25 | 50 | 25 | 1.925 | 3.106 | 3.361 | 21.73 | 36.39 | 41.88 |
| 40 | 50 | 10 | 1.561 | 2.741 | 1.561 | 25.44 | 46.47 | 28.09 |

FTIR spectral characteristic bands belong to the terpolymers given in Table V. Presence of vinylphosphonic acid groups in terpolymers is confirmed by the bands belonging to the vinylphosphonic acid group vibrations. Symmetric and asymmetric O—P—O, and P=O groups in phosphonic acid fragments are characterized by the bands observed at 946–1018 and ~ 1182–1156 $cm^{-1}$ due to the hydrogen bonding between vinylphosphonic acid groups. The anhydride C=O groups are characterized by several bands. The free and hydrogen bonded C=O groups, symmetric, and asymmetric C=O groups, partially hydrolyzed C=O groups and overtones are observed at 1708 and 1963 $cm^{-1}$, respectively. The bands of the aromatic groups are observed at 1450 $cm^{-1}$. Compounds containing —P(O)OH groups show characteristic peaks in the region of 2000–2750 $cm^{-1}$ and the broad peaks resulted from the self-association of the acidic groups. O—H bending vibrations appear at 990 $cm^{-1}$ and broad O—H stretching bands of the free and H-bonded O—H appear at 2500–2900 $cm^{-1}$.

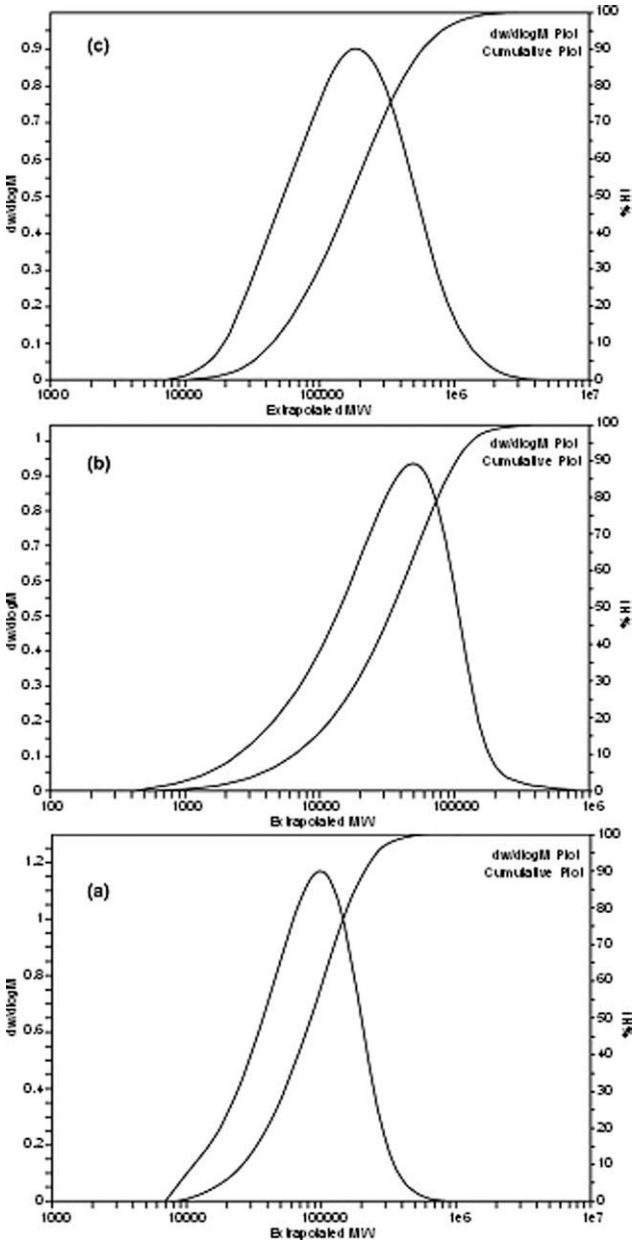


**Figure 3** Molecular weight plots of the terpolymers, (a) terpolymer-1, (b) terpolymer-2, and (c) terpolymer-3.

Figure 4 shows Raman spectra of terpolymers. These regions represent the characteristic peaks of terpolymers coming from maleic anhydride, styrene and vinylphosphonic acid units. The bands between 1100 and 630 $cm^{-1}$ may originate from different vibration modes, belonging to the phosphonic acid units, $PO_2$, $PO_3$, P—C, C—C, and C—O.[35] Peaks at 1005–1007 $cm^{-1}$ and 1037–1043 $cm^{-1}$ correspond to symmetric and asymmetric O—P—O stretching frequency. A peak associated with P=O stretching at 1157–1159 $cm^{-1}$ stands for all the compounds of the phosphonic acid units. A peak at 1199–1220 $cm^{-1}$ is related with the C—O stretching of the maleic anhydride units. Peaks in the range of 1350–1460 $cm^{-1}$ result from $\delta(CH_2)$ on the main chain of terpolymers. A peak at 1604–1609 $cm^{-1}$ may come from the bending frequency water[35] and aromatic ring of

**TABLE IV**
**Average Molecular Weights of the Poly(VPA-*co*-S-*co*-MA)s Obtained by GPC Method**

| Parameter | Terpolymer-1 | Terpolymer-2 | Terpolymer-3 |
|---|---|---|---|
| $\overline{M}_n$ (g $mol^{-1}$) | 53,300 | 13,800 | 101,200 |
| $\overline{M}_w$ (g $mol^{-1}$) | 99,700 | 46,000 | 257,700 |
| $\overline{M}_z$ (g $mol^{-1}$) | 159,800 | 95,900 | 563,300 |
| PDI | 1.87 | 3.32 | 2.55 |
| $R_{gn}$ (nm) | 3.55 | 4.41 | 8.57 |
| $R_{gw}$ (nm) | 3.75 | 4.79 | 10.45 |
| $R_{gz}$ (nm) | 3.94 | 5.13 | 12.60 |

**TABLE V**
**Characteristic FTIR Absorption Bands and Their Assignments for poly(VPA-*co*-S-*co*-MA)**

| Poly(VPA-*co*-S-*co*-MA) absorption band ($cm^{-1}$) | Band assignment |
|---|---|
| 700 (s) | mono-subs benzene ring[44] |
| 763 (s) | mono-subs benzene ring[44] |
| 946 (s) | $\nu_s$ (O—P—O), P—O(H)[36,45] |
| 1006 (s) | $\nu_a$ (O—P—O), P—O(H)[45] |
| 1166 (s) | $\nu_s$ (P=O)[45] |
| 1220 (s) | C—O—C stretching[44] |
| 1437–1495 (s) | $\delta(CH_2)$ scissor, C—H stretching, C=C (aromatic ring)[44,46] |
| 1731 (b) | C=O symmetric[47] C=O asymmetric[48] |
| 1963 (w) | C=O overtone[48] |
| 2335 (w) | POH bending and O—P—O asymmetric stretching[45] |
| 2577 (b) | O—H stretching (H-bonding)[45] |
| 3050–3400 (s) | O—H (H-bonded) —C—H (aromatic ring)[44,47] |
| 3400–3550 (s) | O—H (free)[44] |

s, strong; w, weak; b, broad.

styrene. The bands at 1734 $cm^{-1}$ (weak) assign to stretching of the C=O in the MA unit. C—H, CH=, and O—H bands appeared at 2922–2929 $cm^{-1}$ and 3058–3072 $cm^{-1}$. According to Figure 4 areas of some bands belonging to the vinylphosphonic acid parts increased from (a) to (c).

$^1$H-NMR, $^{13}$C-NMR, and DEPT-135 spectra of terpolymer-1 and terpolymer-2 and the assignments of peaks are presented in Figures 5, 6, and 7 but terpolymer-3 was a tough solid and it was insoluble in common deuterated solvents. Because of this reason NMR spectra were not obtained in solution. By comparison of the $^{13}$C-NMR and DEPT-135 spectra, methine and methylene carbons overlapped. As positive signals indicating the methine carbon, negative signals indicate the methylene carbon atoms in DEPT-135 spectrum. Therefore, $CH_2$ groups of the backbone (VPA) at 34.5 ppm regions appeared as negative signals. However, the integral of the peaks

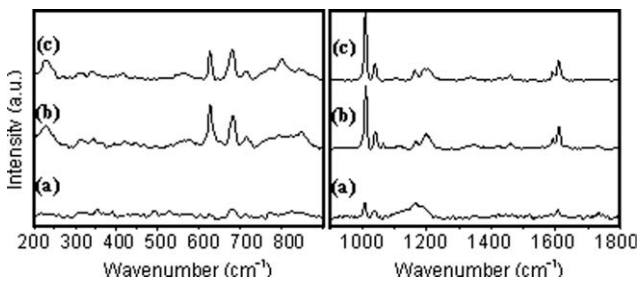


**Figure 4** Raman spectra of terpolymers, (a) terpolymer-1, (b) terpolymer-2, and (c) terpolymer-3, obtained between 200–900 $cm^{-1}$ and 900–1800 $cm^{-1}$ using the 632.8 nm line of a He-Ne laser.

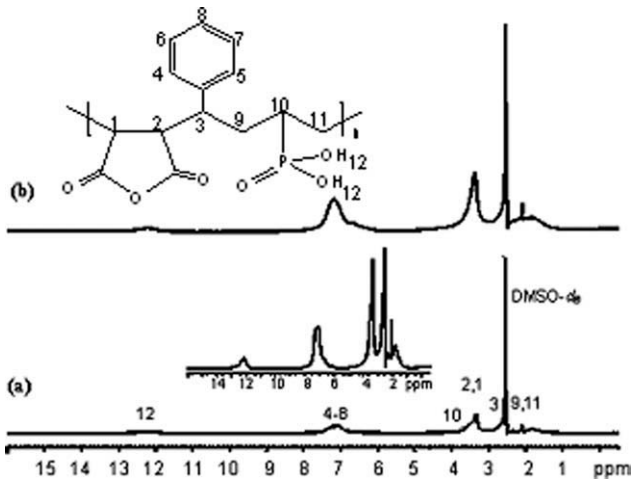


**Figure 5** $^1$H-NMR spectra of terpolymers, (a) terpolymer-1 and (b) terpolymer-2 in DMSO-$d_6$.

at 42.5 ppm regions was reduced to half implying that the peaks belong to the other $CH_2$ group of the backbone (S) of the polymers and are confirmed by DEPT-135 spectra. $^{31}$P-NMR spectra of poly(VPA-*co*-S-*co*-MA)s are presented in Figure 8. Terpolymers show one broad signal at 29.17 and 29.53 ppm, for the terpolymer-1 and terpolymer-2, respectively. Terpolymer-2 which contains more phosphonic acid groups has more intensity than terpolymer-1. These peaks are related to the phosphonic acid groups. The peak at 20.9 ppm in terpolymer-2 may result from the condensation product which results from the inter- or intramolecular interactions between the functional groups.[36,37] The peaks in the region of 11.79 and 11.80 ppm are related to the unreacted or complex bound vinylphosphonic acid monomers.

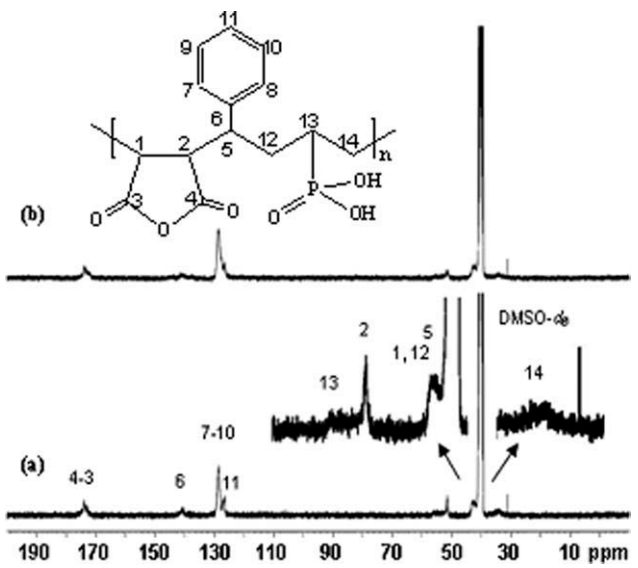


**Figure 6** $^{13}$C-NMR spectra of terpolymers, (a) terpolymer-1 and (b) terpolymer-2 in DMSO-$d_6$.

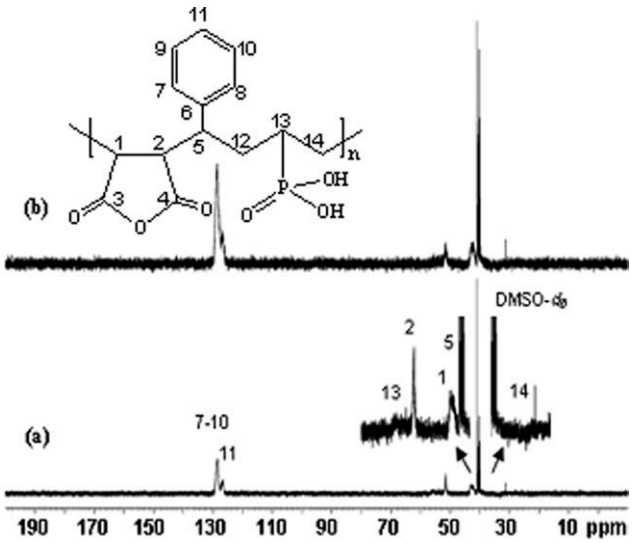


**Figure 7** DEPT-135 NMR spectra of terpolymers, (a) terpolymer-1 and (b) terpolymer-2 in DMSO-$d_6$.

### Thermal properties of terpolymers

Thermal stability of the terpolymers was evaluated by means of TGA measurements. TGA and DTG curves obtained from analysis are shown in Figure 9(a,b). Thermoanalytical results and thermal degradation temperatures are summarized in Table VI. Terpolymers undergo two step decompositions. According to DTG curves, minimum of the first steps are small and the main degradations occur in the second steps. Terpolymers showed small weight loss of 2.6% until 116°C, 2.5% till 105°C and 0.9% till 76°C for terpolymer-1, terpolymer-2, and terpolymer-3 corresponding to a desorption of physically bound water. After these temperatures first degradations occur. These stages appeared at a temperature range of 116–265°C with 27% weight loss for terpolymer-1, temperature range of 107–230°C with 13%

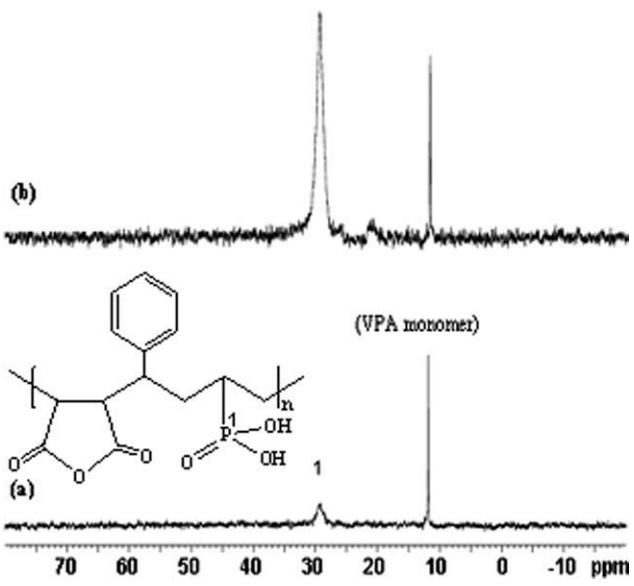


**Figure 8** $^{31}$P-NMR spectra of terpolymers, (a) terpolymer-1 and (b) terpolymer-2 in DMSO-$d_6$.

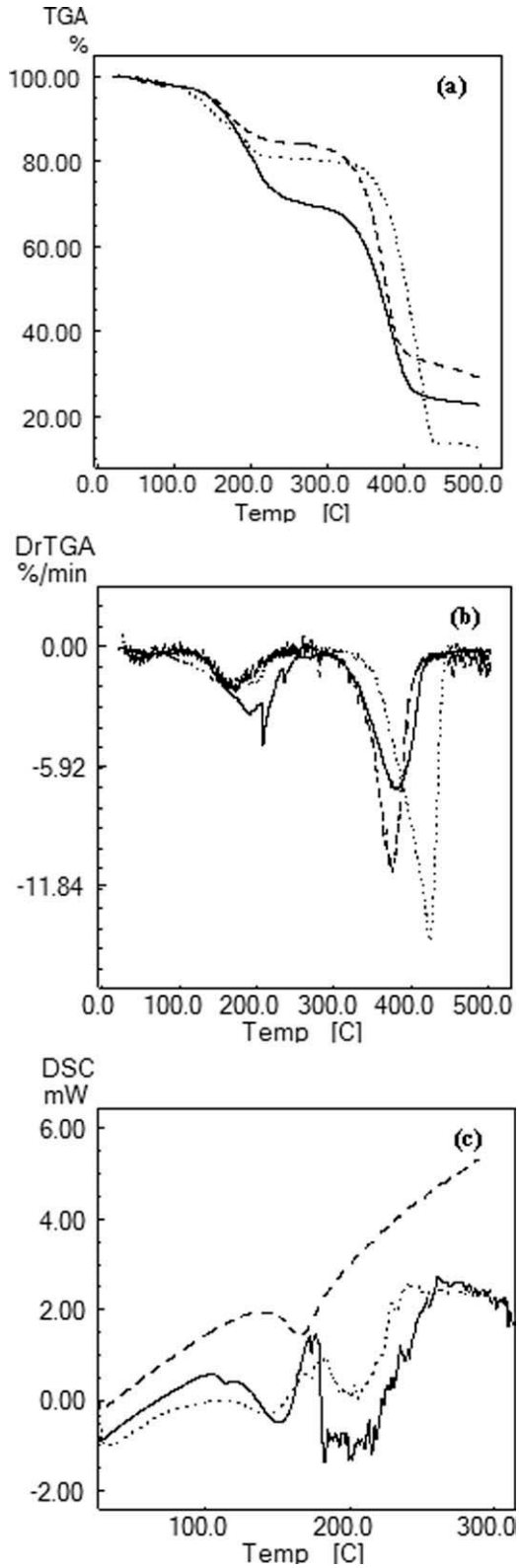


**Figure 9** TGA (a), DTG (b) and DSC (c) curves of the terpolymer-1 (—), terpolymer-2 (---) and terpolymer-3 (···).

**TABLE VI**
**Thermal Behavior of Poly(VPA-*co*-S-*co*-MA)s**

| Terpolymer | VPA unit (mol %) | Weight loss (%) at different temperatures (°C) | | | | | $T_{d1}$ (°C) | $T_{d2}$ (°C) |
|---|---|---|---|---|---|---|---|---|
| | | 100 | 200 | 300 | 400 | 500 | | |
| Terpolymer-1 | 20.55 | 2.1 | 18.7 | 31.1 | 69.8 | 77.3 | 208.4 | 415.4 |
| Terpolymer-2 | 21.73 | 2.3 | 13.4 | 17.0 | 64.4 | 71.1 | 171.2 | 375.7 |
| Terpolymer-3 | 25.44 | 2.0 | 16.6 | 19.8 | 45.9 | 87.5 | 190.2 | 424.4 |

weight loss for terpolymer-2 and temperature range of 78–226°C with 18% weight loss for terpolymer-3, respectively. All terpolymers showed maximum degradation temperature at 208.4, 171.2, and 190.2°C for terpolymers with a small peak minimum. Weight losses in the first steps are associated with water loss from the anhydride formations of phosphonic acid groups and the anhydride formations of partially hydrolyzed maleic anhydride units. In addition, ethylene from the degradation of phosphonic acid units may cause these weight losses.[38,39] At the second step, large weight losses were observed at a temperature range of 295–440°C with 45% weight loss for terpolymer-1, temperature range of 281–444°C with 52% weight loss for terpolymer-2 and temperature range of 329–449°C with 66% weight loss for terpolymer-3, respectively. In the first derivative curves, peaks appeared at 415.4, 375.7, and 424.4°C, for terpolymers. Large weight losses in these second steps may result from the evolution of $CO_2$ gas. Degradations essentially consist of the formation of further anhydride groups by dehydration of P—OH units, main chain degradations, breakdown of C—H bonds and further decompositions of the intermediate macromolecular product. Other degradation products are aromatic fragments of styrene units. Between the ranges of 350–400°C cleavages of the C—P bond occur.[40] Another observation from the TGA curves is the degradation of terpolymers which accelerate quickly when the temperature reaches to about 300°C. Total weight loss of terpolymers is determined as 77.3, 71.1, and 87.5% at 500°C for terpolymers 1, 2, and 3, respectively. Maximum percentage of residue is observed as 28.9% for terpolymer-2. According to Figure 9(a,b) it can be said that terpolymer-3 is thermally stable up to a temperature of about 340°C.

DSC thermograms of terpolymers are presented in Figure 9(c). Terpolymer-1 and terpolymer-3 show glass transitions at 111 and 93°C, respectively. Pseudomelting peaks are observed for all terpolymers and terpolymer-1 and terpolymer-3 show decompositions at about 180°C. For terpolymer-2 no distinct glass transitions were observed up to the pseudomelting temperature because of the ionic crosslinking which results in the restrictions of segmental motions of the terpolymers[41] but it may overlapped with the pseudomelting peak and can be taken as 158°C. This polymer shows no decomposition up to 300°C but other two polymers show degradation starting from the temperature of about 180°C. In poly(VPA-*co*-S-*co*-MA)s containing vinylphosphonic acid substituent, $T_g$ of the terpolymers increased with increasing phosphonic acid concentration from terpolymer 1 to 2 due to the intermolecular hydrogen bonding for terpolymers because this interactions behaved as physical crosslinks and restricted the mobility of the backbone. The reason of the lower $T_g$ of the third terpolymer is the increasing free volume because of a higher bulky vinylphosphonic acid groups and the intramolecular hydrogen bonding between VPA acid groups according to higher content of VPA. This self-association prevents the intermolecular interactions between the MA and VPA units.

### Dynamic mechanical properties of terpolymers

Dynamic mechanical behavior of terpolymer-1 is shown in Figure 10(a). Examination of the storage modulus (SM)-temperature behavior of this terpolymer show broadened low temperature transitions at lower temperatures (−104, −83, and −52°C), indicating possible transitions. From −148 to 167°C, the value of SM decreased from $1.5 \times 10^6$ to $5.6 \times 10^4$ MPa with a sharp drop that starts in the region of 107°C. This sharp peak corresponds to broadened peak at a range of 125–148°C. This peak responds to a glass transition (α-transition). According to loss modulus (LM) two transitions are observed at 125 and 137°C. These transitions result from the α-transition and pseudo\melting behavior of the hydrogen bonded structure. These broadening or multiple peaks indicate that terpolymer is not regular, but it has a random structure. In Figure 10(a) there are three LM peaks at lower temperatures at around 64, −90, and −23°C. These peaks correspond to a secondary or sub-$T_g$ transitions such as β, γ, and δ respectively, in decreasing-temperature order. Sub-$T_g$ transitions are related to the mobility of a relatively small number of monomer units about the chain backbone or to the motion of side chain groups.[42] α-transitions in other DMA parameters are summarized in Table VII. It can be concluded that

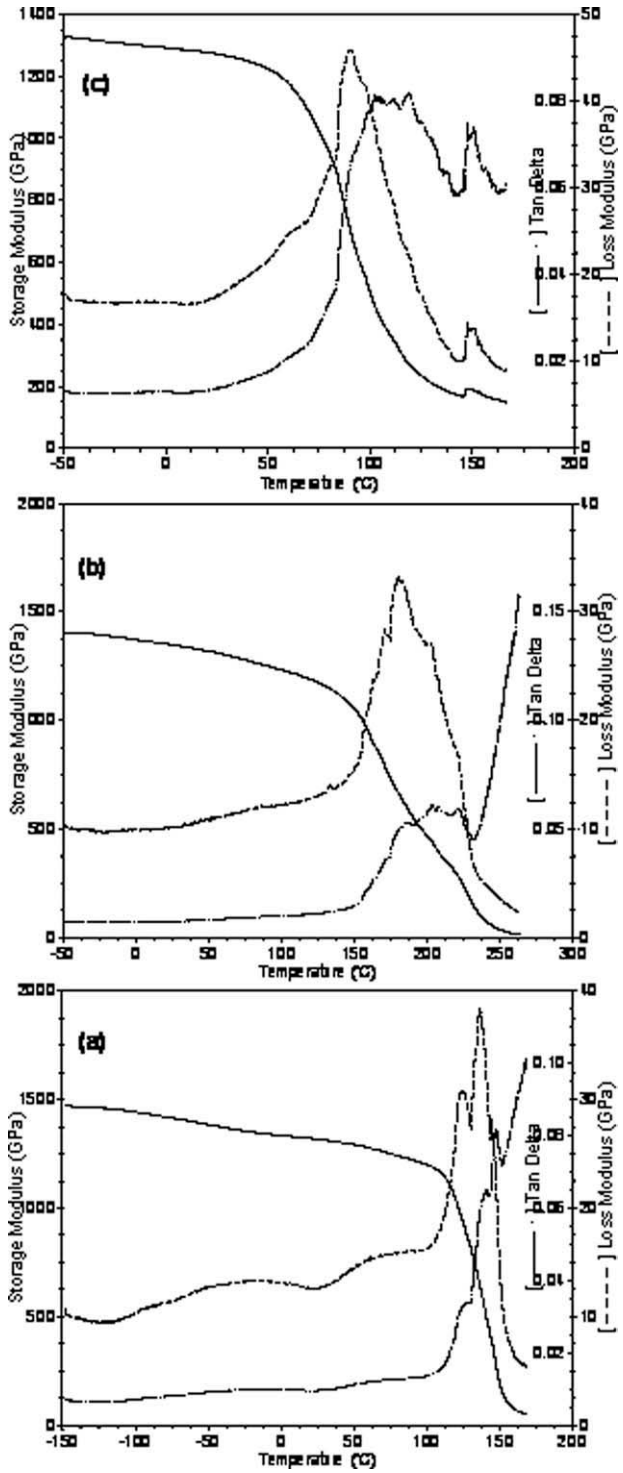


**Figure 10** SM, LM, and tan δ vs. temperature plots of terpolymer-1 (a), terpolymer-2 (b), and terpolymer-3 (c).

all $f(x)$-$x$ functions and derivatives demonstrate nearly the same values for transitions; glass transitions and, pseudomelting behavior of hydrogen bonding units appear around almost the same regions.

DMA curves of terpolymer-2 are presented in Figure 10(b). SM exhibits decrease between the ranges of 130–215°C. SM decreased from $1.4 \times 10^6$ to $1.5 \times 10^4$ MPa (in the temperature range of −48 to 262°C). In the LM-temperature plot one broad peak was observed at 180°C. In tan δ-temperature plot, again a broad peak was observed at about 200°C. These appearing peaks correspond to a glass transition and result from the pseudomelting behavior of hydrogen bonding units, physical crosslinking causing from the hydrogen bonding between functional groups in terpolymer and irregular order of the monomer sequence in terpolymer. Sub-$T_g$ transitions are also observed at low temperatures around −36.81, −25.38, and −6.34°C and correspond to β, γ, and δ transitions, respectively.

DMA properties of terpolymer-3 are presented in Figure 10(c). SM-temperature plot shows a sharp change starting from 40 to 144°C with a decrease in storage modulus from $1.3 \times 10^6$ to $1.7 \times 10^5$ MPa. Glass transition is observed at 87°C, from the SM-temperature plot; at 89°C, from the LM-temperature plot and at 102°C, from the tan δ-temperature plot. In this monomer feed ratio again hydrogen bonded structures of polymer units and different sequences of monomers in terpolymer resulted with broad and shouldered peaks. Secondary transitions were observed in the LM-temperature plot. These transitions come from the mobility around the chain backbone of monomer units and motions of the side chain groups.

All terpolymers show the typical viscoelastic behavior of an amorphous polymer. An observed decrease in SM can be interpreted as a softening of the material. No plateau regions and no relaxation processes in SM were observed above $T_g$. Only, in terpolymer-3, a small peak was observed after α transition but in the LM or tan δ curves, several peaks/transitions were observed at around nearly

**TABLE VII**
**DMA Parameters of Poly(VPA-*co*-S-*co*-MA)s**

| DMA parameters | Terpolymer-1 $T_\alpha$ - relaxation, °C | Terpolymer-2 $T_\alpha$ - relaxation, °C | Terpolymer-3 $T_\alpha$ - relaxation, °C |
|---|---|---|---|
| SM | 123(o) | 135(o) | 72(o) |
| | 147 | 160 | 87 |
| DSM | 122–146[a] | 160–171[a] | 86–89[a] |
| LM | 125–136[a] | 180 | 90 |
| DLM | 128–149[a] | 158–172[a] | 85 |
| DFM | 120–148[a] | 160–171[a] | 86–89[a] |
| tan δ | 125–148[a] | 203 | 102 |
| DV | 125–150[a] | 172–179[a] | 90 |
| DDV | 125–150[a] | 159–173[a] | 85 |

SM, storage modulus; DSM, deriv. storage modulus; LM, loss modulus; DLM, deriv. loss modulus; DFM, deriv. fluxural modulus; DV, dynamic viscosity; DDV, deriv. dynamic viscosity.

[a] Transitions come from glass-transition and pseudomelting resulting from H-bonding overlap; (o), onset.

the same temperatures. Higher transition temperature for the terpolymer-2 may signify that the polymer possesses stronger, or more efficient, dipole–dipole interactions and physical crosslinking of the hydrogen bonded functional groups.[3] Broad peaks may result from the sequential distribution of the comonomers.

### XRD analysis of terpolymers

XRD patterns of poly(VPA-*co*-S-*co*-MA)s are presented in Figure 11. Terpolymers predominantly exhibit amorphous structure having a small peak at $2\theta = 10°$ and a peak at $2\theta = 20°$ depending on the composition and molecular weight of terpolymers. Terpolymer-2 which has relatively lower molecular weight shows higher intensity. This behavior can be explained by intra- and intermolecular hydrogen bonding which may easily form in lower molecular weights.

### Solution properties of terpolymers

Viscosity measurements of the synthesized terpolymers were carried out in the organic solvent (DMF). Terpolymers have ionized or ionizable groups (on the vinylphosphonic acid units) and maleic anhydride units may partially hydrolyze to the maleic acid units. According to Figure 12, terpolymers exhibit typical polyelectrolyte behavior; that is reduced viscosity decreases with an increase in polyelectrolyte concentration. Dissociation of the acidic units is the main factor for this polyelectrolyte behavior. This behavior may also be interpreted such that as the polyelectrolyte concentration decreases; the ionization degree increases and the produced ions form an ionic environment in a size that is higher than the diameter of polymer coil. The repulsion among

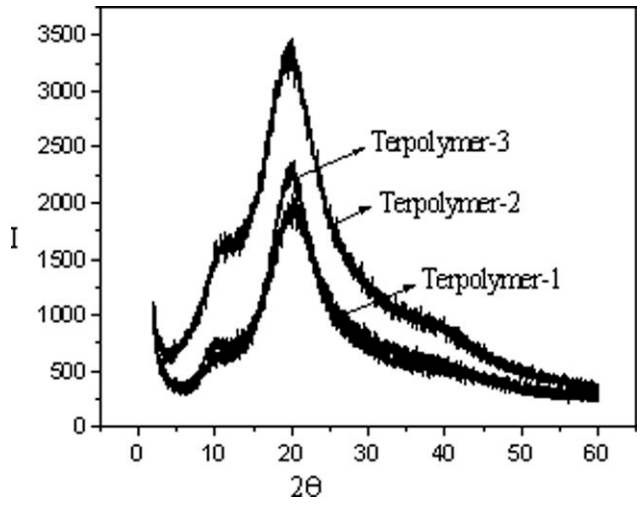


**Figure 11** XRD patterns of terpolymers.

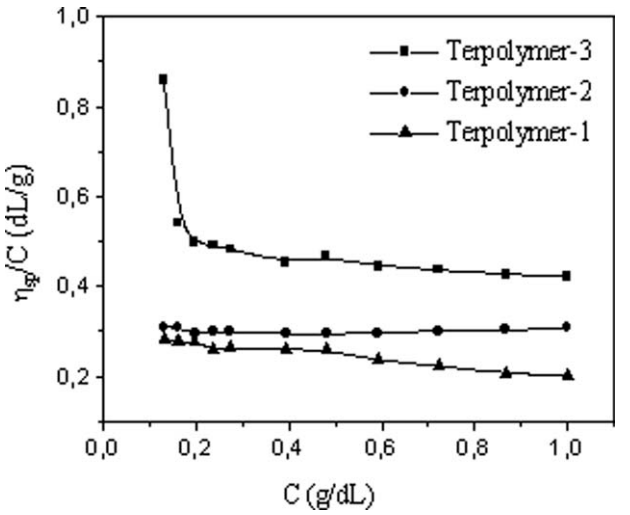


**Figure 12** The plots of $\eta_{sp}/C$ (reduced viscosity) vs. C (concentration) of terpolymers.

the ions increases the rigidity of the chain, expanding the polymeric coil with a consequent increase of the viscosity.[43] Reduced viscosity increases from terpolymer-1 to terpolymer-3 with the increasing VPA content in the comonomer feed solution. This behavior may result from the increasing inter- and intramolecular interactions such as hydrogen bonding with increasing VPA content in terpolymer.

Acid numbers of VPA/St/MA terpolymers were determined experimentally for every sample by the titration method. The results for the terpolymers 1, 2, and 3 were calculated as 302.9, 359.0, and 157.1 mg KOH/g, respectively.

## CONCLUSIONS

This work presents the synthesis and characterization of novel P-containing functional copolymers, which were synthesized by radical-initiated complex-radical terpolymerization of $A_1$(VPA)-D(S)-$A_2$(MA) donor–acceptor monomer system. Complex formations occurred between the acceptor-donor pairs of the VPA-S and MA-S and were confirmed by $^1$H-NMR method. VPA also forms strong H-bonded complex with MA through P—OH. . .O=C— interaction which is confirmed by FTIR and Raman spectroscopy. Both the CTC and H-bonded complex significantly influenced the monomer reactivity ratios in terpolymerization. Terpolymer compositions of VPA, S, and MA in terpolymers were calculated by FTIR, and characterization of terpolymers were completed by different techniques in detail. The results of terpolymer composition–structure–property relations indicate that VPA/S/MA units are randomly distributed along the chain and the functional groups have been confirmed by FTIR, Raman, $^1$H-NMR, $^{13}$C-NMR, DEPT-135, and $^{31}$P-

NMR spectroscopic methods. Terpolymers showed polydispers character with the polydispersities in the range of 1.87–3.32. Thermal stability increased with increasing VPA content up to ~ 400°C. Observed pseudomelting peaks in DSC and in DMA curves can be explained by strong hydrogen bonding phenomena.

The synthesized poly(VPA-*co*-S-*co*-MA)s containing reactive and cross-linkable phosphonic acid and anhydride linkages allow the usage of these terpolymers for the preparation of new generation of metal-complex polymer systems and proton exchange polyelectrolyte membranes, as well as the utilization as effective precursors for the nanosystem and nanomaterial preparations.

The authors thank Prof. Dr. Abidin Temel for kind help in the XRD analysis.

## References


1. Vogl, O. J Macromol Sci Pure Appl Chem 1996, A33, 1571.
2. Erol, İ.; Soykan, C. J Macromol Sci Part A 2002, A39, 405.
3. Wu, Q.; Weiss, R. A. 2004, 42, 3628.
4. Pereira, R. P.; Felisberti, M. I.; Rocco, A. M. Polymer 2006, 47, 1414.
5. Nicholson, J. W.; Singh, G. 1996, 17, 2023.
6. Eom, G. T.; Oh, S. Y.; Park, T. G. J Appl Polym Sci 1998, 70, 1947.
7. Alexandratos, S. D.; Strand, M. A.; Quillen, D. R.; Walder, A. J. Macromolecules 1985, 18, 829.
8. Selzer, R. B.; Howery, D. G. Macromolecules 1986, 19, 2673.
9. Sata, T.; Yoshida, T.; Matsusaki, K. J Membr Sci 1996, 120, 101.
10. Sata, T.; Sata, T. Jr; Yang, W. J Membr Sci 2002, 206, 31.
11. Ebdon, J. R.; Price, D.; Hunt, B. J.; Joseph, P.; Gao, F.; Milnes, G. J.; Cunliffe, L. K. Polym Degrad Stabil 2000, 69, 267.
12. Medyakova, L. V.; Rzaev, Z. M. O.; Güner, A.; Kibarer, G. J Polym Sci Polym Chem 2000, 38, 2652.
13. Rzaev, Z. M. Maleic Anhydride Polymers and Copolymers; Elm Baku, 1984 (in Russian); Chem Abstr 102, 11410w, 1985.
14. Cowie, J. M. G. Alternating Copolymers; Plenum Press: New York, 1985.
15. Culbertson, B. M. Encycl Polym Sci Eng 1985, 275, 9.
16. Hill, D. T. J.; O'Donnell, J. H.; O'Sullivan, P. W. Prog Polym Sci 1982, 8, 215.
17. Ratzsch, M.; Vogl, O. Prog Polym Sci 1991, 16, 279.
18. Rzaev, Z. M. O. Prog Polym Sci 2000, 25, 163.
19. Florjanczyk, Z.; Krawiec, W. J Polym Sci Part A Polym Chem 1989, 27, 4099.
20. Rzaev, Z. M. O. J Polym Sci Part A Polym Chem 1999, 37, 1095.
21. Yang, J. Z.; Otsu, T. Macromolecules 1992, 25, 102.
22. Florjanczyk, Z.; Krawiec, W.; Such, K. J Polym Sci Polym Chem 1990, 28, 795.
23. Zhongqing, H.; Zhicheng, Z.; Guixi, Z.; Weijun, L. Polymer 2005, 46, 12711.
24. Keramopoulos, A.; Kiparissides, C. J Appl Polym Sci 2003, 88, 161.
25. Shoonbrood, H. A.; Reijen, B. V.; Kock, J. B. L.; Manders, B. G.; Herk, A. M.; German, A. I. Macromol Rapid Commun 1995, 16, 119.
26. Boback, M.; Kowollic, C. Macromol Chem Phys 1999, 200, 1764.
27. Dube, M. A.; Penlidis, A. Macromol Chem Phys 1995, 196, 1101.
28. Gao, J.; Penlidis, A. Macromol Chem Phys 2000, 201, 1176.
29. Brauer, G. M.; Horowitz, E. In Analytical Chemistry of Polymers; Kline, G. M., Ed.; Interscience Publishers: New York, 1962; p III/82–85.
30. Hanna, M.; Ashbaugh, J. J Phys Chem 1964, 68, 811.
31. Tsuchida, E.; Tomano, T.; Sano, H. Macromol Chem 1972, 151, 245.
32. Rzaev, Z. M.; Bryksina, L. V.; Sadikh-Sade, S. I. J Polym Sci Polym Symp 1973, 42, 519.
33. Jaacks, V. V. Macromol Chem 1967, 105, 289.
34. Rzaev, Z. M. O.; Güner, A.; Kibarer, G.; Kaplan Can, H.; Aşıcı, A. Eur Polym J 2002, 38, 1245.
35. Archanjo, B. S.; Carvalho, L. A. S.; Rassa, M.; Miquita, D. R.; Oliveira, F. A. C.; et al. J Nanosci Nanotechnol 2007, 7, 1.
36. Millaruelo, M.; Steinert, V.; Komber, H.; Klopsch, R.; Voit, B. Macromol Chem Phys 2008, 209, 366.
37. Bingöl, B.; Meyer, W. H.; Wagner, M.; Wegner, G. Macromol Rapid Commun 2006, 27, 1719.
38. Chan, H. S. O.; Ng, S. C.; Ho, P. K. H. Macromolecules 1994, 27, 2159.
39. Nagarajan, R.; Tripathy, S.; Kumar, J.; Bruno, F. F.; Samuelson, L. Macromolecules 2000, 33, 9542.
40. Parvole, J.; Jannasch, P. Macromolecules 2008, 41, 3893.
41. Erdemi, H.; Bozkurt, A. Eur Polym J 2004, 40, 1925.
42. Lee, S. Y. NASA Technical Memorandum, 1990, 100758.
43. Rivas, B. L.; Pereira, E. D.; Moreno-Villoslada, I. Prog Polym Sci 2003, 28, 173.
44. Erdik, E. Organik Kimyada Spektroskopik Yöntemler; Gazi Kitabevi: Ankara, 1998.
45. Thomas, L. C. Interpretation of the Infrared Spectra of Organophosphorous Compounds; Heyden: New York, 1974.
46. Lin-Vien, D.; Colthup, N. B.; Fately, W.G.; Graselli, J. G. Infrared and Raman Charactersitic Frequencies of Organic Molecules; Academic Press: California, 1991.
47. Sanmathi, C. S.; Prasannakumar, S.; Sherigara, B. S. Bull Mater Sci 2004, 27, 243.
48. Devrim, Y.; Rzaev, Z. M. O.; Pişkin, E. Macromol Chem Phys 2006, 207, 111.